

Thermoelectricity in natural and synthetic hydrogelsBrandon R. Brown,^{*} Mary E. Hughes,[†] and Clementina Russo*Department of Physics, University of San Francisco, 2130 Fulton Street, San Francisco, California 94117, USA*

(Received 30 July 2003; revised manuscript received 13 January 2004; published 30 September 2004)

We describe a technique for measuring a Seebeck effect in gels and present data for three systems. Notably distinct signals are obtained for gel originating in the electrosensitive organs of marine sharks, synthetic collagen-based gel, and as a control, seawater, the gels' solvent. Only the gel of sharks shows a reversible thermoelectric signal. The difference between gel samples and seawater simply confirms that gels suppress mass transport. The difference between synthetic gel and the gel of sharks shows that the charged polymers of the shark gel restrict mass transport much more successfully than the polymers of the collagen gel, and we submit that this sort of ion localization is key to the emergence of thermoelectricity in a gelatinous substance. We compare the properties of the natural gel to those of established thermoelectrics.

DOI: 10.1103/PhysRevE.70.031917

PACS number(s): 87.68.+z, 82.70.Gg, 72.20.Pa, 87.19.Bb

INTRODUCTION

Gel characteristics combine certain qualities of liquids and solids. Polymer hydrogels, in particular, are known to contain up to 99% water solvent [1], suggesting liquidlike physical properties. However, the polymer matrix gives rise to unique structural properties, with volumes that exhibit tunable sensitivity to various environmental factors, including electric fields [2]. Such properties have resulted in both an ever-expanding array of applications for polymer hydrogels and an increased appreciation for their role in living systems [3,4].

While significant thermoelectric effects have been documented in amorphous materials [5] and organic solids [6], such effects are not typically associated with gels. In particular, the Seebeck effect phenomenologically exhibits a voltage gradient in response to an applied temperature gradient within a material.

We recently reported an apparent thermoelectric mode of sensory transduction in the electrosensitive organs of sharks; the hypothesis depends on a thermoelectric signal in an extracellular hydrogel filling the electrosensitive organ [7]. Here we describe a gel thermopower measurement, rule out systematic effects, and investigate the physical phenomenon of thermoelectricity in an organic hydrogel. This includes measurements for hydrogels collected from sharks, hydrogels synthesized in house, and, for comparison, "blank cells" of liquid seawater. In order to investigate the role of ion concentration, we also present data at diluted salt concentrations for the liquid seawater and synthesized gel samples.

The electrosensors in sharks, skates, and rays (the elasmobranchs) are the most exquisite sensors of electric fields known in nature [8], and they are simultaneously the most exquisite sensors of thermal fluctuations [9]. Distant freshwater relatives like the paddlefish utilize these organs for detecting zooplankton prey [10], and marine sharks utilize

these organs to detect the weak electric fields given off by more macroscopic prey [11]. The electrosensitive organs, the ampullae of Lorenzini, are small innervated bulbs linked to the creature's surface by canals. Both the ampullae and the canals are filled with a clear, homogeneous hydrogel.

The gel consists of 97% water by weight, with dissolved salts at concentrations matching seawater [12]. The precise structure of the gel glycoproteins is still unknown, but they are hydrophilic and heavily sulfated, suggesting an effective negative charge [13]. Electrophoresis has shown that the glycoproteins range in size from 20 to 200 kilodaltons [14]. The bulk hydrogel has shown room-temperature conductivity and temperature-dependent conductivity that correspond to a semiconductor [14]. This led naturally to the question of thermoelectricity, as semiconductors exhibit significant Seebeck coefficients. In addition to the proposal that this biological hydrogel possesses a non-negligible thermopower [7], we also note that a thermoelectric mechanism for cooling was recently proposed in the chitin-based cuticle of an insect [15].

EXPERIMENT

Samples of the natural hydrogel are collected from shark specimens *post mortem*. The collection, handling, and storage of the gel have been described elsewhere [14]. The gel has proven robust in the face of thermal and electrical cycling in previous experiments.

Our technique to explore gel thermoelectricity uses a typical open-circuit configuration employed for solids. However, while accurate thermoelectric measurements are difficult for solids [16], measurements for a gel include additional complications. The experimental configuration is shown in Fig. 1. Work in a vacuum is impossible, so we enclose samples in quartz. Hence, while experiments with solids can measure temperature and electric potential simultaneously at one position on a sample, our thermometers are slightly removed from the sample; this contributes significantly to reported uncertainties.

A 1 ml quartz cuvet is carefully filled with gel using a 1 ml syringe and an 18-gauge needle to minimize air bubbles

^{*}Electronic address: brownb@usfca.edu

[†]Present address: Division of Engineering and Applied Sciences, Harvard University, 29 Oxford St., Cambridge, MA 02138, USA.

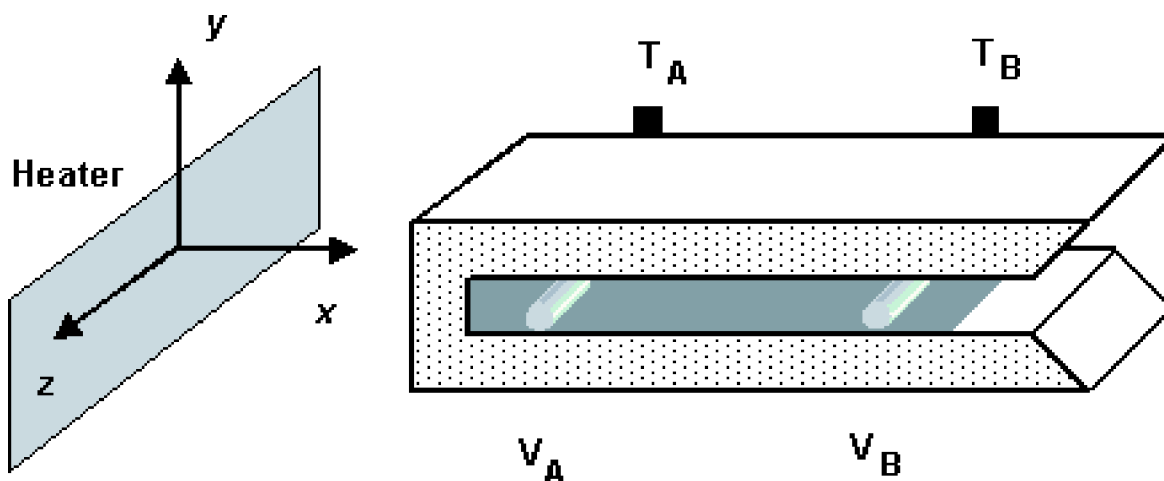


FIG. 1. Sample chamber. A gel sample is shown in gray. Two platinum thermometers are attached via thermal grease to the thin sides of the cuvet, and two braided metallic leads (insulated but for their tips) run into the cuvet to sit adjacent to the thermometer positions. The x axis is horizontal.

in the sample. The open cuvet is then sealed with silicon putty. Two voltage leads are made of braided platinum wire and placed 2.5 cm apart within the gel. Voltage is monitored with a Keithley 2182 nanovoltmeter. The samples exhibit a resting voltage due primarily to large and asymmetric contact resistances at the metal-gel interfaces. These offsets are specific to a given pair of platinum leads and vary with the ion content (and thereby the resistance) of the samples. Most of the data presented here were collected with one set of leads, for which the trial-to-trial voltage offsets were between -8 and $+1$ mV for each loading of shark gel, between -20 and 0 mV for synthetic and seawater samples, and between -120 to -40 mV for comparator samples of reduced ion content. Variation of the offset between sample loadings is attributed to variations in the residual air pockets that remain against the braided leads. These offsets were fairly steady hours after loading a sample, but tiny nonzero drifts were usually present. Data were collected only when such a drift was both negligible in magnitude and also measurably constant before heating.

Two platinum thermometers are mounted on a thin-walled side of the quartz cuvet, each one adjacent to one of the voltage contacts. The long ends of the cuvet are then encased in quartz blocks of at least 1.0 cm thickness (extending in y and z in Fig. 1), with thermal grease connecting the cuvet to the quartz and filling the empty regions near the Pt thermometers. Heater wire is shaped into a thin two-dimensional heating plate, $3\text{cm} \times 1\text{cm}$, to promote parallel, planar thermal fronts throughout the sample chamber. This plate was alternately mounted at either of the small ends of the quartz cuvet to establish thermal gradients in alternate directions. The heater and thermometers are monitored by a Lakeshore 330 digital temperature controller, with roughly 0.27 W of power promoting temperature gradients between -0.2 and $+0.2$ K between the voltage leads. Each sample was reloaded and voltage leads were replaced three times. Heat is applied for a variable time (20–180 s) and the resulting temperature and voltage gradients are monitored.

To further investigate the technique, the signal, and the notion of hydrogel thermoelectricity, collagen-based hydro-

gel comparator samples were synthesized with seawater as a solvent, and seawater solutions were used for “blank cell” measurements. Both the synthetic hydrogel and seawater samples possess ion concentrations, dc conductivities, and activation energies nearly identical to those of the shark gel. Activation energies were obtained by measuring dc conductivity over a range of temperatures, as previously described [14]. To assess the import of dissolved salts in these systems, liquid and synthetic gel samples were also prepared using seawater diluted with deionized water. While the conductivities decreased as salts were removed, the activation energies did not change appreciably, suggesting that all samples in this work shared the same transport mechanism.

Before presenting results, we must address legitimate concerns of signal artifacts. The voltage measurements here involve nontrivial metal-gel or metal-solution interfaces; in electrochemistry, the interface gives rise to the so-called “double layer” of differentiated ion and solvent concentrations [17], while in condensed matter physics, the interface can be considered a Schottky barrier. Metal-solution interfaces are known to have inherent potentials, and these potentials can vary with temperature to the extent of hundreds of microvolts per degree kelvin [18,19]. In short, one may argue that the measured signals reside predominantly at the platinum-sample interfaces, giving very little information about the bulk sample between the platinum leads.

Despite such misgivings, a number of experimental aspects indicate that the gel signal is significant and largely independent of interface electrochemistry. First, the technique is non-faradaic, and the leads have never had voltages applied to them. Even in strong electrolyte solutions, documented interactions for an active platinum interface require at least 400 mV to drive them [18]. Second, data employing silver leads, as shown in previous work, gave approximately the same results for the shark gel as platinum leads [7]. Standard electrochemical cell potentials for solutions are strongly metal-specific [19]. Third, while seawater and the shark gel have nearly identical ion concentrations and water contents, their signals show opposite signs of $\Delta V/\Delta T$ during heating. Finally, the inclusion of bubbles between leads in the gel

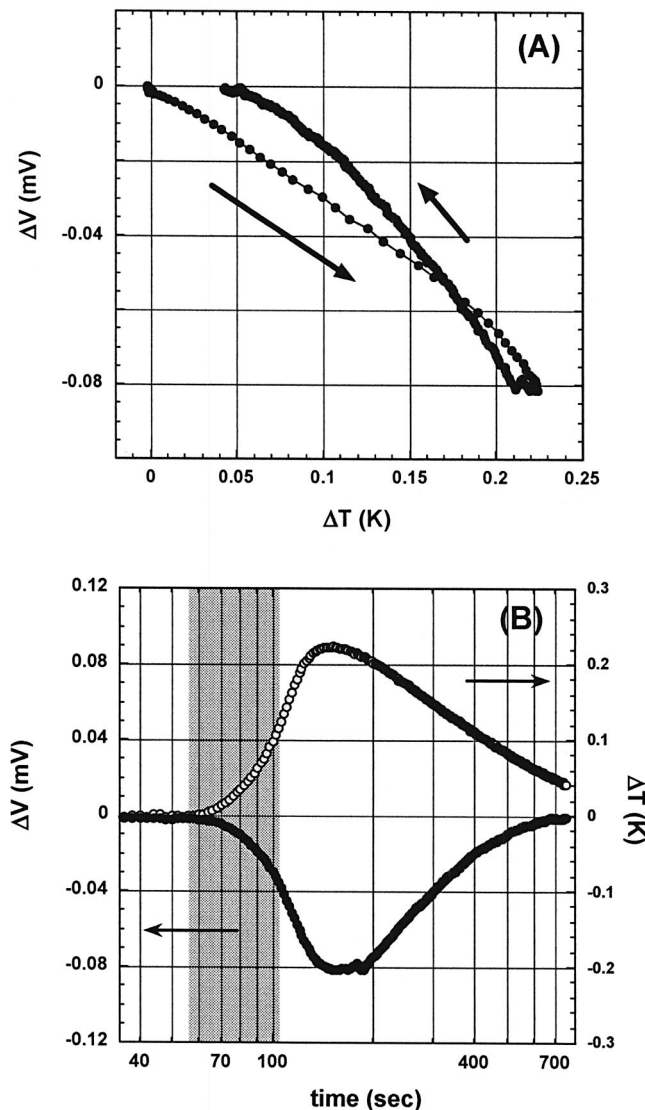


FIG. 2. Typical data trace collected from the ampullary gel of *Carcharodon carcharias*. (a) Potential gradient versus thermal gradient with data points plotted at two-second intervals. Trace begins at origin and follows effects of heating (large arrow) and cooling (small arrow). (b) Both gradients monitored versus time in a semi-log format, with the gray region denoting heating. Filled circles denote ΔT , and open circles ΔV , as indicated by the arrows. The original voltage offset of 0.33 mV, due to contact asymmetry, has been subtracted, and a dc voltage drift of 70 nV/s (observed before heating) has been removed.

noticeably alters the resulting data. If the signal resided primarily at the interfaces, alterations of sample far from the leads should have a relatively minor effect.

RESULTS

Data for the gel of *Carcharodon carcharias*, a white shark, are shown in Fig. 2(a). The relative duration of the heating and cooling cycles is shown in Fig. 2(b). The entire process appears reversible. The slope of $\Delta V/\Delta T$ is independent of both heating rate and total ΔT range (from 0.05–0.5

K). These characteristics lead us to refer to the effect as a thermopower.

From the $\Delta V/\Delta T$ obtained during heating, a Seebeck coefficient S is derived. For an open circuit measurement between two leads at points A and B ,

$$\Delta V = \int_{T_B}^{T_A} S_{\text{leads}}(T) dT - \int_{T_B}^{T_A} S_{\text{sample}}(T) dT, \quad (1)$$

where the metallic leads have established S values [20]. Assuming that S values are roughly constant with temperature for gradients under 1 K, we simplify to a typical open-circuit thermopower expression:

$$S_{\text{sample}} \cong S_{\text{leads}} - (\Delta V/\Delta T), \quad (2)$$

where $S_{\text{Pt}} = -5.3 \mu\text{V/K}$, for instance [20]. Using Pt leads, as we did for the data in Fig. 2, we find $S_{\text{gel}} = +290 \pm 70 \mu\text{V/K}$ for the white shark gel, while for Ag leads, we found $240 \pm 50 \mu\text{V/K}$ [7]. The positive S values of the gel fit with the notion of proton transfer as a transport mechanism, and the values are comparable to undoped semiconductors [20].

Data for comparator samples are strikingly different from those of the shark gel. Data for a liquid seawater sample appear in Fig. 3(a). The traces show both an effect opposite to that observed in shark gel and also a repeatable hysteresis; the extent of the hysteresis is roughly proportional to the range of ΔT . The lack of correlation between ΔV and ΔT is demonstrated by the way they evolve in time [Fig. 3(b)]. Note that we do not expect the thermometers to reflect the exact temperature of the leads for a fluid sample due to convection. However, as the ΔV and ΔT peaks are separated by more than two minutes [Fig. 3(b)], we believe the hysteresis to be a real effect, separate from a thermometer-lead offset.

Fluid samples were also prepared with diluted salt content by mixing seawater with deionized water. The data in Fig. 3(c) compare pure seawater to a sample diluted to 2.5% seawater. The more dilute sample exhibits the hysteresis to a lesser extent.

We quantify the relaxation feature, or the return, simply by defining a phenomenological measure $R \equiv (\Delta V_{\text{max}} - \Delta V_0)/\Delta T_{\text{max}}$ where ΔV_0 is the original voltage offset before heating. For a given sample, this is roughly constant to within 20% for all ΔT_{max} values greater than 0.08 K (for ΔT less than 0.08, we seldom find a measurable ΔV response, and we believe that this is due to the thermometers finding a temperature offset within the quartz that is not manifest for any appreciable time within the liquid sample).

Data for synthesized collagen gels appear in Fig. 4. These data combine features of those from shark gel and seawater, showing the same sign of a thermoelectric signal as the shark gel during heating followed by a hysteretic return. Once again, at reduced ion concentrations, the magnitude of the return feature is suppressed.

A summary of the results appears in Table I. Seebeck coefficients are reported for samples where the slope of $\Delta V/\Delta T$ during heating was independent of ΔT , and the uncertainties are standard deviations after multiple (8–10) trials. We present S values for the synthetic gel with some

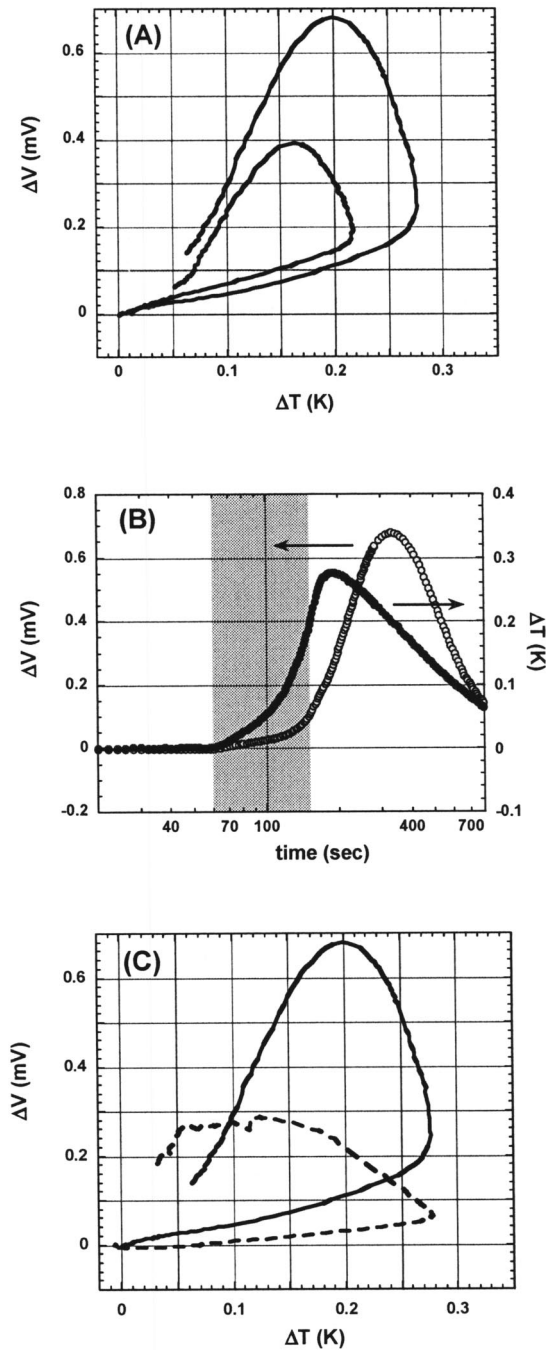


FIG. 3. Data for blank cells of seawater solutions. (a) Potential versus thermal gradients for seawater during two separate heating cycles (each data run follows counter-clockwise development). (b) Outer data set from (a) shown versus time on a semilog plot with gray region denoting heating. Filled circles denote ΔT , and open circles ΔV , as indicated by the arrows. (c) Data for pure seawater compared to a solution of 2.5% seawater in deionized water (dashed trace). Original voltage offsets (circa -20 mV for full ion concentrations and -100 mV for diluted samples) were removed, and dc drifts of about $0.1 \mu\text{V/s}$ were removed.

hesitation; the effect is not at all reversible, as it is in the shark gels, but for the sake of argument, the collagen gels display a repeatable, linear thermoelectric signal during heating. The magnitude of the hysteretic return, R , is given only

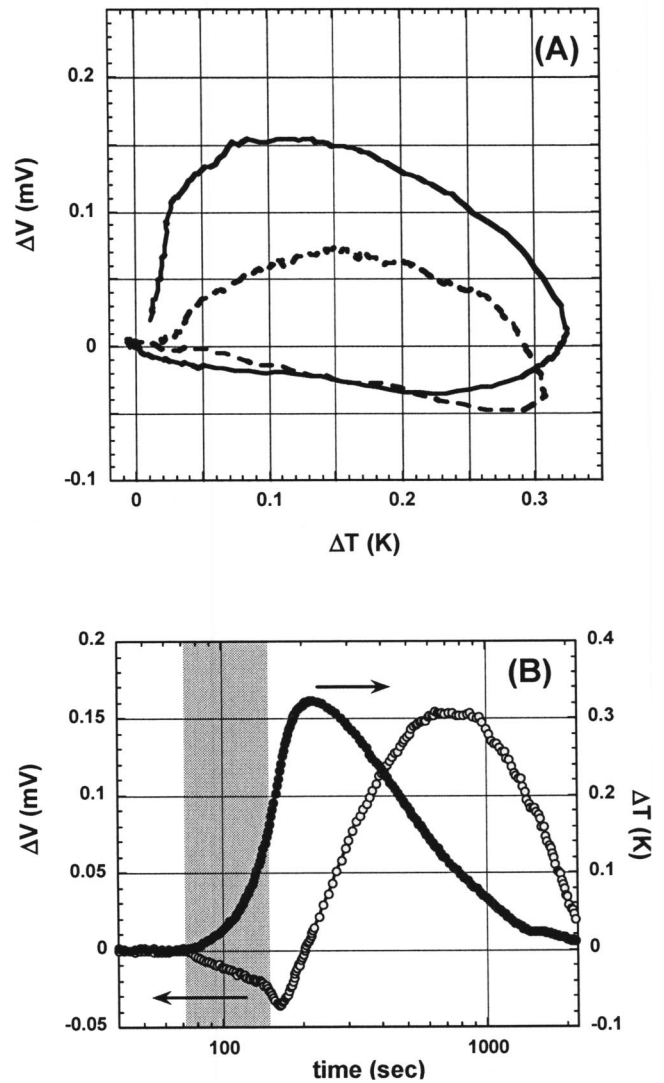


FIG. 4. (a) Potential versus thermal gradients for both synthesized collagen gel with ion content of seawater (solid trace) and for a diluted gel containing 2.5% seawater (dotted trace). As with the fluid data, each trace runs counter-clockwise. (b) Data for nondiluted gel shown versus time on a semilog plot, with gray region denoting heating. Filled circles denote ΔT , and open circles ΔV , as indicated by the arrows. Original voltage offsets (circa -20 mV for full ion concentrations and -100 mV for diluted samples) were removed.

to demonstrate two points: the return is much larger in liquid samples than in the synthetic gel samples; and the return magnitude decreases when the ion content of a sample is decreased.

DISCUSSION

Despite sharing nearly equivalent ion concentrations, electrical conductivities, and activation energies, the white shark gel, the undiluted synthetic collagen hydrogel, and undiluted seawater samples give distinct signals in our experiments. Only the white shark gel exhibits a reversible, linear signal that we are comfortable describing as a thermopower.

TABLE I. Summary of results. Four-terminal conductivity measurement technique and derivation of activation energy described elsewhere [14]. R described in text.

| Sample | σ at 298 K (S/m) | E_A (kJ/mol) | S ($\mu\text{V/K}$) | R ($\mu\text{V/K}$) |
|---------------------------------------|-------------------------|----------------|-------------------------|-------------------------|
| White shark gel | 3.15 ± 0.1 | 16.2 ± 0.5 | $+290 \pm 70$ | NA |
| Collagen gel, 100% seawater solvent | 4.80 ± 0.1 | 16.2 ± 0.3 | $+270 \pm 60$ | 540 |
| Collagen gel, 10% seawater solvent | 0.72 ± 0.04 | 16.3 ± 0.4 | $+220 \pm 80$ | 330 |
| Collagen gel, 2.5% seawater solvent | 0.26 ± 0.02 | 16.0 ± 0.4 | $+200 \pm 70$ | 270 |
| Seawater solution, full concentration | 5.20 ± 0.2 | | | 3000 |
| Seawater solution, 2.5% concentration | 0.30 ± 0.05 | | | 1400 |

While we describe fluid seawater as a blank cell for these experiments, the term is misleading in that the thermal and electrical physics of a salt-filled liquid are arguably more sophisticated than that in a well-ordered hydrogel. Mass transport within the sample space provides a sensible explanation for the observed hysteresis (Fig. 3). Only small shifts in local ionic density would be needed to give sub-mV voltage perturbations. We believe such shifts occur primarily through ion migration. Though convection may be present, it presumably transports the bulk liquid as a neutral whole that would not give a net voltage signal.

Ignoring convective effects, the seawater's ion migration and subsequent asymmetries of ionic density can be understood in the following manner. For constant pressure and uniform electric fields, the temperature dependence of the chemical potential for a given ionic species, μ_i , may ideally be written as

$$\mu_i = \mu_{i0} + RT \ln(x_i), \quad (3)$$

where μ_{i0} is the chemical potential of the pure ionic species and x_i is its mole fraction [21]. Equation (3) is only accurate for very dilute solutions, and it does not account for the presence of multiple species. As $x_i < 1$ for all species, μ_i will decrease with increasing temperature. Migration follows, as ions move toward lower μ_i values. Different species encounter different magnitude gradients based on their x_i values, with more dilute species facing greater $\Delta\mu_i$. Furthermore, absolute ionic mobilities u_i vary significantly from ion to ion in water, so different ions will respond to their μ_i gradients to different extents, and we expect a net, nonzero ion migration flux density J :

$$J = - \sum_i c_i u_i \left(\frac{\Delta\mu_i}{s} \right), \quad (4)$$

where c_i denotes ion concentration, s is the spatial extent of our cell, and J is given in units of moles/m²s [21]. This can be converted to an effective electrical current density via the electric charge of each species. Mobilities and mole fractions for the components of seawater are available (in order of abundance, the most significant species are Cl⁻, Na⁺, Mg²⁺, SO₄²⁻, Ca²⁺, and K⁺) [17]. Our zeroth order calculations, using ideal parameters for the six most abundant ions, give a negative current, but we find the calculation to be extremely sensitive to mole fraction and mobility values. To accurately model the seawater sample to the

extent of predicting voltage signals, one would need to move past the simple form of Eq. (3) to determine μ_i gradients, since seawater is not especially dilute and since many species are present. In addition, the absolute mobilities available in the literature are collected from single ion, dilute solutions, environments obviously unlike seawater. In sum, we fully expect a net ion migration current and a corresponding voltage signal between the leads. Removing the thermal gradient would then leave the ionic gradient (and hence the voltage gradient) to slowly relax via diffusion. This picture qualitatively matches the blank cell data of Fig. 3.

The fact that our phenomenological R depends on ion concentration supports the ion migration picture. While decreasing ion content by factors of 10 and 25 in Eq. (4) would suggest a more substantial signal reduction than that shown in Table I, we note that reduced concentrations actually increase the chemical potential gradients and thereby the net migration forces. In addition, R is much smaller in the synthetic gels than in solutions (with a respective ratio of about 1 to 5.5), indicating reduced ion mobilities within the ordered water of a hydrogel, as expected [4]. Finally, a comparison of the time scales for seawater and synthetic gel also suggests ion migration [see Figs. 3(b) and 4(b)]; as mobilities are lower in a hydrogel than in a pure fluid, the time range is increased. In seawater, the ΔV peak trails the ΔT peak by 144 s, while in the synthetic hydrogel, the lag time is 543 s. These two data sets have nearly identical heating times, and the samples have nearly identical ion concentrations.

The return feature has not been observed for the shark gels. This suggests that the shark gel orders its solvent and localizes its dissolved salts to a greater extent than the collagen gels. The effectively negative polymer gel of cellular cytoplasm has shown a strong preference for localizing positive ions [4], and the shark gel arguably will do the same, since it is heavily sulfated. Once mass migration and convection are suppressed, the sample is presumably "solid enough" for something like conventional thermoelectricity in a solid to be manifest.

At a basic level, the Seebeck effect arises from a free energy asymmetry for charge carriers between relatively warm and cool regions [20], and such a condition is plausible in a gel if convection and migration are absent. The temperature dependence of the hydrogel, as previously measured [14], matches the Arrhenius behavior of a semiconductor. Charge carriers in such a sample are thermally activated, so the free energy landscapes for carriers within both semicon-

ductors and the shark hydrogel are extremely sensitive to thermal gradients. That sensitivity leads naturally to the possibility of significant thermoelectric effects. That being said, the detailed, lattice-based models for solids are presumably inappropriate [16], and further theoretical work will be required for gels.

The thermoelectric effect found in an insect's cuticle material recommends a comparison of the shark polymer to the chitin polymer; though S has not been directly measured in that system, it is inferred to be roughly 2 mV/K [15]. Chitin, one of the most abundant polysaccharides in nature, contains glucosamine, as does the organic material in the shark gel [13]. However, the acetyl groups of chitin render it more electrically neutral than what one would presume for the sulfate-rich polymers in sharks. A much greater understanding of the shark gel polymers is needed to move beyond speculation.

Phenomenologically, if gelatinous materials truly sustain thermoelectric effects, they should be intriguing candidates for thermoelectric cooling or other applications. To compare the natural hydrogel to accepted thermoelectrics, we estimate the dimensionless figure of merit, ZT ,

$$ZT = \frac{S^2 \sigma T}{\lambda}, \quad (5)$$

where σ and λ are electrical and thermal conductivity respectively [16]. Assuming a λ of 0.6 W/mK, in keeping with a generic value for tissue, and using σ and S values reported here, the shark gel shows $ZT \sim 0.0003$ at room temperature. A ZT approaching or above 1.0 is desirable for thermoelectric applications. However, the effect of altering salt content in a hydrogel can obviously enhance its electrical conductivity and perhaps alter its effective S value (e.g., see Table I). In this way, a hydrogel's figure of merit could hypothetically be increased.

While it is unclear which thermoelectric solids, if any, are appropriate for comparison to the gel results, quasicrystals would be more appropriate than crystals, since they lack long-range translational order. For instance, $A_{107.8}Pd_{20.9}Mn_{8.3}$ is considered worthy of future study as a thermoelectric [22]. While it has a relatively low room-

temperature ZT value of 0.08, it has a relatively high room-temperature S value of 80 μ V/K [22]. In comparison, the hydrogel estimates for ZT are lower, but their S values are substantially higher.

In sum, the data presented above confirm the existence of a thermoelectric effect in the hydrogel collected from the electrosensors of sharks, and they suggest that ion localization within a hydrogel is crucial to the thermoelectric signature. Previously, we suggested that the electrosensor's observed sensitivity to temperature acceleration reflected an actual sensitivity to temperature gradients [7]. In closing, we note the experiments of Akoev *et al.*, who monitored the effect of several stimuli on the firing rates of nerves leading from the electrosensors of anesthetized skates [23]. In one case, they applied a pointlike heat source to different positions along the gel-filled canal attached to the skate's electrosensor. Heat applied to the midpoint of the canal (4 centimeters away from the sensing cells) created the *opposite* transient effect on nerve firing rates as heat applied directly to the sensing cells, even though both experiments raised the overall temperature of the electrosensor. Considering the gel-filled canal, those experiments obviously generated temperature gradients of opposing directions, and according to our data, electric field gradients of opposing directions. It is in no way clear how other mechanisms of temperature sensation could begin to address those data [24]. Akoev *et al.* also found that each electrosensitive organ's sensitivity to temperature fluctuations was directly proportional to that organ's electrical sensitivity [23]. Something within the organ intimately connects electrical and thermal fluctuations, and the data presented here point to thermoelectricity as the most convincing (if not the only) candidate.

ACKNOWLEDGMENTS

This work was supported in part by grants from the Fletcher Jones Foundation and the National Science Foundation (DUE Grant No. 87960). Access to white shark specimens provided by Sean Van Sommeran of the Pelagic Shark Research Foundation. We thank Alexis Abramson, John C. Hutchison, Larry Margerum, and Ali Zahn for fruitful discussions.

-
- [1] Y. Osada and J. Gong, *Prog. Polym. Sci.* **18**, 187 (1993).
 - [2] T. Tanaka, I. Nishio, S-T. Sun, and S. Ueno-Nishio, *Science* **218**, 467 (1982).
 - [3] A. S. Hoffman, *Clin. Mater.* **11**, 13 (1992).
 - [4] G. H. Pollack, *Cells, Gels, and the Engines of Life* (Ebner & Sons, Seattle, 2001).
 - [5] P. Kounavis, P. A. Vomvas, E. Mytilineou, M. Roilos, and L. J. Murawski, *J. Phys. C* **21**, 967 (1988).
 - [6] Y. W. Park, A. Denenstien, C. K. Chiang, A. J. Heeger, and A. G. MacDiarmid, *Solid State Commun.* **29**, 747 (1979).
 - [7] B. R. Brown, *Nature (London)* **421**, 495 (2003).
 - [8] R. W. Murray, *J. Exp. Biol.* **39**, 119 (1962).
 - [9] A. Sand, *Proc. R. Soc. London, Ser. B* **125**, 524 (1938).
 - [10] P. E. Greenwood, L. M. Ward, D. F. Russell, A. Neiman, and F. Moss, *Phys. Rev. Lett.* **84**, 4773 (2000).
 - [11] A. Kalmijn, *Nature (London)* **212**, 1232 (1966).
 - [12] R. W. Murray and W. Potts, *Comp. Biochem. Physiol.* **2**, 65 (1961).
 - [13] J. Doyle, *Biochem. J.* **103**, 325 (1967).
 - [14] B. R. Brown, J. C. Hutchison, M. E. Hughes, D. R. Kellogg, and R. W. Murray, *Phys. Rev. E* **65**, 061903 (2002).
 - [15] J. S. Ishay, V. Pertsis, E. Rave, A. Goren, and D. J. Bergman, *Phys. Rev. Lett.* **90**, 218102 (2003).
 - [16] G. S. Nolas, J. Sharp, and H. J. Goldsmid, *Thermoelectrics: Basic Principles and New Materials Developments* (Springer, New York, 2001).

- [17] A. J. Bard and L. R. Faulkner, *Electrochemical Methods* (Wiley, New York, 1980).
- [18] A. Wieckowski, *Interfacial Electrochemistry* (Dekker, New York, 1999).
- [19] G. Milazzo and S. Caroli, *Tables of Standard Electrochemical Potentials* (Wiley, New York, 1978).
- [20] S. O. Kasap, *Principles of Electronic Materials and Devices*, 2nd ed. (McGraw-Hill, New York, 2001).
- [21] J. O. Bockris and A. K. N. Reddy, *Modern Electrochemistry, Volume 1: Ionics* (Plenum, New York, 1998).
- [22] A. J. Pope, T. M. Tritt, M. A. Chernikov, and M. Feuerbacher, *Appl. Phys. Lett.* **75**, 1854 (1999).
- [23] G. N. Akoev, N. O. Volpe, and G. G. Zhadan, *Comp. Biochem. Physiol. A* **65**, 193 (1980).
- [24] H. A. Braun, K. Schafer, and H. Wissing, in *Thermoreception and Thermoregulation*, edited by J. Bligh and K. Voigt (Springer-Verlag, New York, 1990).